Bias-Aware Bayesian Filtering Using Gaussian Process Latent Force Models

E. Lourens[1(✉)] and Ø. W. Petersen[2]

[1] Delft University of Technology, Faculty of Civil Engineering and Geosciences, Delft, The Netherlands
e.lourens@tudelft.nl

[2] NTNU, Department of Structural Engineering, Taipei City, Taiwan
oyvind.w.petersen@ntnu.no

Abstract. An important consideration when using sequential Bayesian filters for the estimation of unknown states and inputs, is the potential impact of modelling errors on the accuracy and precision of the estimation. When the modelling errors are explicitly accounted for in the estimation, one can speak of bias-aware filtering. One approach that has been suggested to achieve bias-aware filtering is the use of Gaussian process latent force models. Using this approach, the biases are represented as Gaussian processes and identified from the vibration data in conjunction with the additional unknown quantities. In this contribution, we focus on modelling biases due to miscalibrated dynamic properties in linear system models. We analyze the treatment of such biases using Gaussian process latent force models, and explore the robustness of the approach to changes in sensor configurations using simulated data from a cantilever beam.

Keywords: Bayesian filtering · Modelling error · Gaussian process latent force models

1 Introduction

Sequential Bayesian filters are becoming increasing popular to solve various estimation problems in structural dynamics, ranging from load estimation and virtual sensing to parameter identification and damage detection. An important characteristic of these filters is that both modelling and measurement errors are explicitly modelled as stochastic variables. The means and covariances of these error fields are thus assumed known. Due to a lack of information, however, these error fields are in practice often inaccurately specified. This leads to suboptimal estimates [1], as well as difficulties when trying to interpret the uncertainties associated with these estimates. In this contribution, the focus is on modelling uncertainties that manifest as miscalibrated dynamic properties. This includes uncertainties related to damping, joint or soil stiffnesses, boundary conditions, environmental influences, etc. While difficult to characterize in terms of a mean and covariance, these uncertainties could have strong impacts on the estimation results in a filtering context.

Á. Cunha and E. Caetano (Eds.): EVACES 2025, LNCE 674, pp. 322–331, 2025.
https://doi.org/10.1007/978-3-031-96110-6_30

Existing approaches used in the treatment of modeling bias can be classified into 1) those aiming to account for the bias in the statistics [1–4], 2) those aiming to explicitly identify the bias [5–7], and 3) those aiming to explicitly identify as well as model the bias [8]. The latter category has received little attention in structural dynamics, and is addressed in this contribution through the development of a bias-aware estimator based on corrective Gaussian process latent forces. The presented work can be related to recent developments by Kashap [9] and Rogers [10], with an important difference that additional unknown inputs to the (linear) system are accounted for.

2 Bias-Aware Filtering by Means of Gaussian Process Latent Force Models

As shown in [11], modal property errors can be captured in an unmodelled force residual, which may be linearized as follows:

$$\overbrace{\ddot{\mathbf{z}} + 2\boldsymbol{\Omega}_\mathrm{e}\boldsymbol{\Xi}_\mathrm{e}\dot{\mathbf{z}} + \boldsymbol{\Omega}_\mathrm{e}^2\mathbf{z} = \boldsymbol{\Phi}_\mathrm{e}^\mathrm{T}\mathbf{S}_\mathrm{p}\mathbf{p}(t)}^{\text{Modelled dynamics}} \overbrace{+\Delta\boldsymbol{\Phi}^\mathrm{T}\mathbf{S}_\mathrm{p}\mathbf{p}(t) - 2\boldsymbol{\Omega}_\mathrm{e}\Delta\boldsymbol{\Omega}\mathbf{z} - (2\boldsymbol{\Omega}_\mathrm{e}\Delta\boldsymbol{\Xi} + 2\boldsymbol{\Xi}_\mathrm{e}\Delta\boldsymbol{\Omega})\dot{\mathbf{z}}}^{\text{Unmodelled force residual}} \quad (1)$$

where $\dot{\mathbf{z}}$ and $\ddot{\mathbf{z}}$ represent the modal velocities and accelerations, $\boldsymbol{\Omega}$ and $\boldsymbol{\Xi}$ are the modal frequency and damping matrices, and a distinction is made between true and erroneous properties and the underlying perturbation according to $\mathbf{X} = \mathbf{X}_\mathrm{e} + \Delta\mathbf{X}$. Considering the modal bias forces separately, one can write:

$$\ddot{\mathbf{z}} + 2\boldsymbol{\Omega}_\mathrm{e}\boldsymbol{\Xi}_\mathrm{e}\dot{\mathbf{z}} + \boldsymbol{\Omega}_\mathrm{e}^2\mathbf{z} = \boldsymbol{\Phi}_\mathrm{e}^\mathrm{T}\mathbf{S}_\mathrm{p}\mathbf{p}(t) + \begin{bmatrix} p_{\mathrm{bias},1}(t) \\ p_{\mathrm{bias},2}(t) \\ \vdots \\ p_{\mathrm{bias},\mathrm{n_m}}(t) \end{bmatrix} \quad (2)$$

2.1 Latent Force Models

As also shown in [11], each of the unmodelled force residuals in (2) can be characterized by increased energy around a certain frequency. This motivated the design of a Gaussian process latent force model (LFM), defined here for a single modal bias force, with the following autocorrelation function (ACF) [12]:

$$R_{p_\mathrm{bias}}(\tau) = \sigma_p^2 \exp(-\lambda|\tau|)\cos(\omega_0\tau) + \delta(\tau)\sigma_\eta^2 \quad (3)$$

Apart from the specification of a dominant frequency component ω_0, the function in Eq. (3) allows for adjusting, through a fading factor λ, how far in the frequency spectrum the amplitudes are influenced. To account for possible disturbances along the entire frequency axis, the white noise term $\delta(\tau)\sigma_\eta^2$ is added.

If $p_{\text{bias}}(t)$ is modelled as a stationary GP with the ACF presented in Eq. (3), it can be considered as an output from a latent force model in state-space form as follows:

$$\begin{bmatrix}\dot{s}_1(t)\\ \dot{s}_2(t)\end{bmatrix} = \begin{bmatrix}-\lambda & -\omega_0\\ \omega_0 & -\lambda\end{bmatrix}\begin{bmatrix}s_1(t)\\ s_2(t)\end{bmatrix} + \begin{bmatrix}1 & 0\\ 0 & 1\end{bmatrix}\begin{bmatrix}w_1(t)\\ w_2(t)\end{bmatrix} \tag{4}$$

$$p_{\text{bias}}(t) = \begin{bmatrix}1 & 0\end{bmatrix}\begin{bmatrix}s_1(t)\\ s_2(t)\end{bmatrix} + \eta(t) \tag{5}$$

where w_1 and w_2 are uncorrelated white noise driving inputs that will have variance $\sigma^2_{w_1} = \sigma^2_{w_2} = 2\lambda\sigma^2_p$. Here, the variables s_1 and s_2 are latent states capturing the oscillatory dynamics around a center frequency ω_0. The structure of the state matrix in Eq. (4) is similar to a single degree of freedom damped oscillator, since its eigenvalues are given by $-\lambda \pm i\omega_0$. Note again also the additional white noise term $\eta(t)$ with corresponding variance σ^2_η included in Eq. (3).

This latent force model is defined by four hyperparameters (per modal bias force): σ_p, λ, ω_0, σ_η. Through the optimization of these hyperparameters, relative weights can be assigned to the periodic versus white noise components of the force residual.

In the case of $\mathrm{n_m}$ modal bias forces – cf. Eq. (2) – the state-space model in Eq. (4) and (5) can be expanded by gathering the individual LFM's as block diagonals:

$$\dot{\mathbf{s}}(t) = \mathbf{F}_\mathrm{c}\mathbf{s}(t) + \mathbf{L}_\mathrm{c}\mathbf{w}(t) \tag{6}$$

$$\mathbf{p}_{\text{bias}}(t) = \mathbf{H}_\mathrm{c}\mathbf{s}(t) + \boldsymbol{\eta}(t) \tag{7}$$

where $\mathbf{F}_\mathrm{c} \in \mathbb{R}^{2\mathrm{n_m}\times 2\mathrm{n_m}}$, $\mathbf{L}_\mathrm{c} \in \mathbb{R}^{2\mathrm{n_m}\times 2\mathrm{n_m}}$, and $\mathbf{H}_\mathrm{c} \in \mathbb{R}^{\mathrm{n_m}\times 2\mathrm{n_m}}$, are constructed as:

$$\mathbf{F}_\mathrm{c} = \begin{bmatrix}\mathbf{F}_{\mathrm{c},1} & & \\ & \ddots & \\ & & \mathbf{F}_{\mathrm{c},\mathrm{n_m}}\end{bmatrix},\ \mathbf{L}_\mathrm{c} = \begin{bmatrix}\mathbf{L}_{\mathrm{c},1} & & \\ & \ddots & \\ & & \mathbf{L}_{\mathrm{c},\mathrm{n_m}}\end{bmatrix},\ \mathbf{H}_\mathrm{c} = \begin{bmatrix}\mathbf{H}_{\mathrm{c},1} & & \\ & \ddots & \\ & & \mathbf{H}_{\mathrm{c},\mathrm{n_m}}\end{bmatrix} \tag{8}$$

and the blocks $\mathbf{F}_{\mathrm{c,j}}$, $\mathbf{L}_{\mathrm{c,j}}$, and $\mathbf{H}_{\mathrm{c,j}}$ is defined for each targeted mode j according to Eqs. (4) and (5).

2.2 Augmented Formulation

A conventional state-space model in modal coordinates (the modelled dynamics) can now be augmented with a state-space model for multiple modal bias forces (the unmodelled residual). More specifically, the state-space representation of (1), with only the modelled dynamics included and $\mathbf{x}(t) = [\mathbf{z}(t)\ \dot{\mathbf{z}}(t)]^\mathrm{T}$, is augmented with (6) and (7) as follows:

$$\begin{bmatrix}\dot{\mathbf{x}}(t)\\ \dot{\mathbf{s}}(t)\end{bmatrix} = \begin{bmatrix}\mathbf{A}_{\mathrm{c,e}} & \mathbf{B}_\mathrm{c}^{\text{bias}}\mathbf{H}_\mathrm{c}\\ \mathbf{0} & \mathbf{F}_\mathrm{c}\end{bmatrix}\begin{bmatrix}\mathbf{x}(t)\\ \mathbf{s}(t)\end{bmatrix} + \begin{bmatrix}\mathbf{B}_{\mathrm{c,e}}\\ \mathbf{0}\end{bmatrix}\mathbf{p}(t) + \begin{bmatrix}\mathbf{0}\\ \mathbf{L}_\mathrm{c}\end{bmatrix}\mathbf{w}(t) + \begin{bmatrix}\mathbf{B}_\mathrm{c}^{\text{bias}}\\ \mathbf{0}\end{bmatrix}\boldsymbol{\eta}(t) \tag{9}$$

where the matrix $\mathbf{B}_{\mathrm{c}}^{\mathrm{bias}} = \begin{bmatrix} \mathbf{0} \\ \mathbf{S}_{\mathrm{m}} \end{bmatrix}$ assigns bias correction forces to the modes specified in $\mathbf{S}_{\mathrm{m}}$. For instance, if bias correction forces are included for all modes in the model, then $\mathbf{S}_{\mathrm{m}} = \mathbf{I}$. Again, the subscript e is used to indicate erroneous model matrices.

To couple the measured observations to the bias-aware state Eq. (9), an augmented observation equation is defined as:

$$\mathbf{y}(t) = \begin{bmatrix} \mathbf{G}_{\mathrm{c,e}} \; \mathbf{J}_{\mathrm{c}}^{\mathrm{bias}} \mathbf{H}_{\mathrm{c}} \end{bmatrix} \begin{bmatrix} \mathbf{x}(t) \\ \mathbf{s}(t) \end{bmatrix} + \mathbf{J}_{\mathrm{c,e}} \mathbf{p}(t) + \mathbf{J}_{\mathrm{c}}^{\mathrm{bias}} \boldsymbol{\eta}(t) \tag{10}$$

where $\mathbf{J}_{\mathrm{c}}^{\mathrm{bias}} = \begin{bmatrix} \mathbf{0} \\ \mathbf{S}_{\mathrm{a}} \boldsymbol{\Phi} \mathbf{S}_{\mathrm{m}} \end{bmatrix}$ is again used to assign the bias correction forces to the affected modes.

The continuous-time model of Eqs. (9) and (10) is discretized as in e.g. [13]. Additional white sensor noise characterized by a covariance matrix $\mathbf{R}_v$ (usually diagonal) is then added to the observation Eq. (10). In the discrete-time model, the following covariance matrices appear for the augmented system:

$$\mathbf{Q}_{\mathbf{a}} \approx \Delta t \begin{bmatrix} \mathbf{B}_{\mathrm{c}}^{\mathrm{bias}} \mathbf{Q}_{\eta} \left(\mathbf{B}_{\mathrm{c}}^{\mathrm{bias}} \right)^{\mathrm{T}} & \mathbf{0} \\ \mathbf{0} & \mathbf{L}_{\mathrm{c}} \mathbf{Q}_{w} \mathbf{L}_{\mathrm{c}}^{\mathrm{T}} \end{bmatrix} \tag{11}$$

$$\mathbf{R}_{\mathbf{a}} \approx \frac{1}{\Delta t} \left[\mathbf{J}_{\mathrm{c}}^{\mathrm{bias}} \mathbf{Q}_{\eta} \left(\mathbf{J}_{\mathrm{c}}^{\mathrm{bias}} \right)^{\mathrm{T}} \right] + \mathbf{R}_{v} \tag{12}$$

$$\mathbf{S}_{\mathbf{a}} \approx \begin{bmatrix} \mathbf{B}_{\mathrm{c}}^{(\mathrm{bias})} \mathbf{Q}_{\eta} \left(\mathbf{J}_{\mathrm{c}}^{(\mathrm{bias})} \right)^{\mathrm{T}} \\ \mathbf{0} \end{bmatrix} \tag{13}$$

where $\mathbf{Q}_{\mathbf{a}}$, $\mathbf{R}_{\mathbf{a}}$, and $\mathbf{S}_{\mathbf{a}}$ represents the covariance matrices of the augmented states, observations, and their cross-covariance, respectively. The driving white noise processes have diagonal covariance matrices:

$$\mathbf{Q}_{\eta} = \begin{bmatrix} \sigma_{\eta,1}^2 & & \\ & \ddots & \\ & & \sigma_{\eta,\mathrm{n_m}}^2 \end{bmatrix}, \quad \mathbf{Q}_{w} = \begin{bmatrix} \sigma_{w_1,1}^2 & & \\ & \ddots & \\ & & \sigma_{w_2,\mathrm{n_m}}^2 \end{bmatrix} \tag{14}$$

2.3 Hyperparameter Optimization

The hyperparameters consists of the set $\{\sigma_p, \lambda, \omega_0, \sigma_\eta\}$ for each mode, i.e. a total of $4 \cdot \mathrm{n_m}$ variables. These are optimized through a procedure of maximum log-likelihood using the augmented state space model developed in Sect. 2.2 and the measurement data. Equations for the log-likelihood will be presented in a forthcoming paper and are omitted here for brevity, but can be maximized through standard gradient-based algorithms.

Note that for each iteration in such an optimization, state and input estimation needs to be performed to obtain the estimates $\hat{\mathbf{x}}_{\mathbf{a}}(t)$ and $\hat{\mathbf{p}}(t)$. This is, however, quick for linear systems where Kalman-type algorithms for state and input estimation are run in their steady-state configuration.

3 Numerical Examples

The bias-aware filter presented in the previous section is now applied in a numerical example with a cantilever beam, where also its performance using data from various sensor configurations is explored.

3.1 System Model and Excitation

A finite element model of a cantilever beam is constructed using 20 elements – see Fig. 1. The properties of the beam are $L = 10$ m, $E = 210$ GPa, $I = 10^6$ mm^4, and $m = 100$ kg/m. A discrete time step of $\Delta t = 0.01$ s is used.

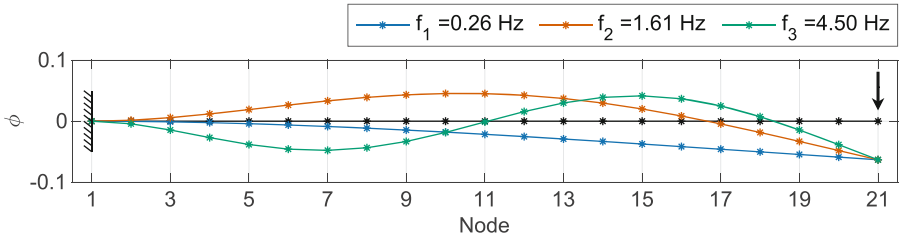

Fig. 1. The finite element model of the beam and its first 3 modal frequencies and shapes.

A reduced-order modal model of the beam is built using the three lowest modes shown in Fig. 1. Modal damping is set to 1%. The beam is excited by a logarithmic sine sweep applied at the tip:

$$p(t) = \sin\left(2\pi f_{\text{start}} \cdot \frac{\exp(gt) - 1}{g}\right), \quad g = \frac{\log(f_{\text{end}}/f_{\text{start}})}{T_{\text{sweep}}} \tag{15}$$

This force covers the range from $f_{\text{start}} = 0.1$ Hz to $f_{\text{end}} = 6$ Hz, which will in turn excite all 3 modes of interest. The sweep time is set to $T_{\text{sweep}} = 300$ s. Note that the location of the force is known to the filter, while its time history is unknown and estimated in conjunction with the bias forces. The beam's response to this force – $\mathbf{y}(t)$ – is simulated in the time domain using the exact dynamic properties presented in Fig. 1. This emulates the dynamic response of the "real" structure that is, by definition, error-free.

Noise is added to the system as follows: the sensor noise is characterized by $\mathbf{R}_v = 10^{-8}\mathbf{I}$, leading to signal-to-noise ratios in the order of $10^3 - 10^4$. In addition, a small amount of background white noise excitation is added to each mode with variance 10^{-4} (see [14] for a formulation of noise covariance matrices).

3.2 Bias-Aware Estimation

State and input estimation is now performed using an erroneous model, where the modal characteristics of the beam are perturbed as follows:

- The 3 natural frequencies are scaled by 0.95, 1.05, and 0.95, respectively.
- The modal damping in all three modes is scaled by 2, since damping tends to have higher relative uncertainties.
- The mode shapes are scaled by $\sqrt{1.1}$, $\sqrt{0.9}$, and $\sqrt{1.1}$, corresponding to a ± 10 % error on the modal mass.

Initially, results are presented for an estimation based on acceleration data collected at node 11 (midspan) and 21 (tip, collocated with force), as well as displacement data collected at node 16 (3/4 span). To optimize the hyperparameters of the bias-aware filter (12 in total), *fmincon* in Matlab was used. For each mode, initial values were set as $\sigma_p = 10^{-2}$, $\sigma_\eta = 10^{-5}$, and $\lambda = 0.1\omega_0$, where the central frequency ω_0 was initially guessed as the (erroneous) natural frequency. Results are presented in Figs. 2, 3, and 4 for the modal states, identified external forces, and bias forces, respectively. In these figures a distinction is made between the *exact* results (without any estimation performed), and the estimation results obtained with the *true* model, the *erroneous* model, and the *bias-aware* case, i.e. the erroneous model, but including unknown bias forces.

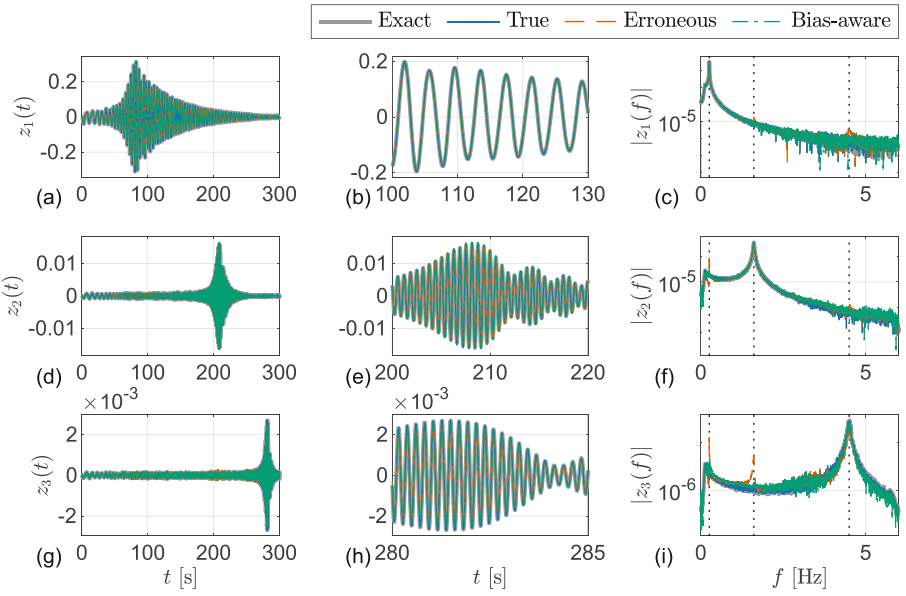

Fig. 2. Exact modal states compared to those estimated using the different models, with and without bias compensation.

The modal states are well captured in all cases, with only minor artifacts present in the 2nd and 3rd mode at the true natural frequencies (dashed lines). The good performance at the level of the modal states is expected, since the identified external force is compensating for the model errors. In Fig. 3 the force

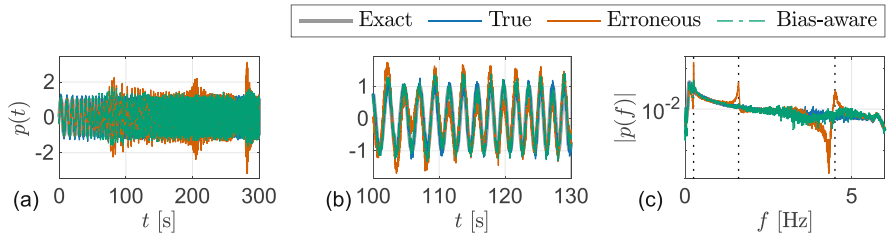

Fig. 3. Exact external forces compared to those estimated using the different models, with and without bias compensation.

identified using the erroneous model clearly shows amplifications around the true natural frequencies. This is, however, not the case for the bias-aware estimation, where the model errors are separately accounted for through the bias forces.

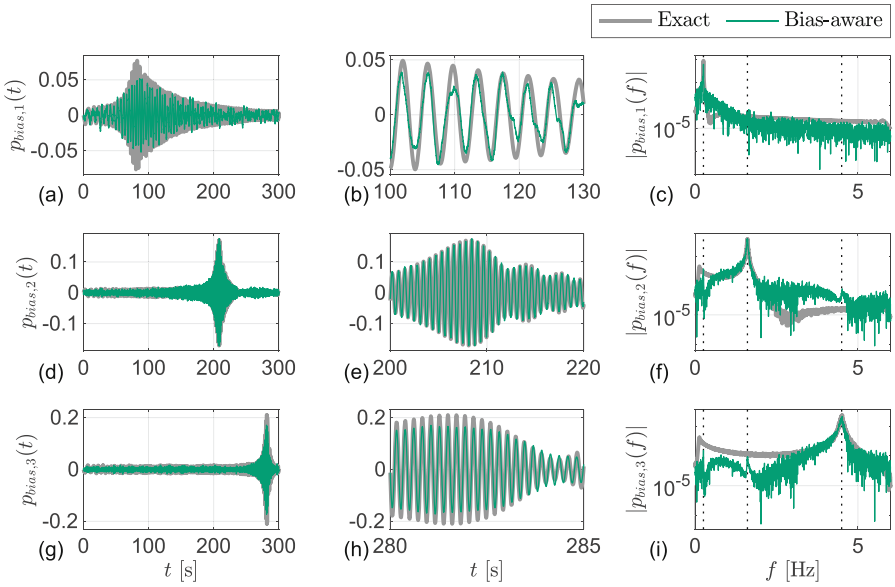

Fig. 4. The exact and estimated bias forces.

The estimated bias forces can indeed be seen to peak around the true natural frequencies in Fig. 4. This implies that the unknown, true modal frequencies were successfully recovered through the hyperparameter optimization procedure for each GP bias force. This recovery of the dynamics of the true system is quantified in Table 1, where the value obtained for the hyperparameter representing the natural frequency, ω_0, is compared to its true value for each of the modes.

Table 1. Optimized hyperparameters ω_0 vs. true natural frequencies in rad/s

	True ω_i	Optimized ω_0	Error [%]
Mode 1	1.611	1.597	<1
Mode 2	10.098	9.839	2.6
Mode 3	28.273	27.977	1

3.3 Sensitivity to Sensor Configurations

In this section, the sensitivity of the results to changes in the sensor configuration is assessed. The displacement sensor is kept fixed at node 16, while the accelerometers are placed in different configurations as indicated on the horizontal and vertical axes in Fig. 5. For simplicity, the optimized hyperparameter values from the original configuration of Sect. 3.2 are used in all analyses. To facilitate a quick comparison between the results obtained with different configurations, the normalized root mean square error is computed for each modal state as well as the external force:

$$\text{NRMSE} = \sqrt{\frac{\sum (z(t) - \hat{z}(t))^2}{\sum z(t)^2.}} \tag{16}$$

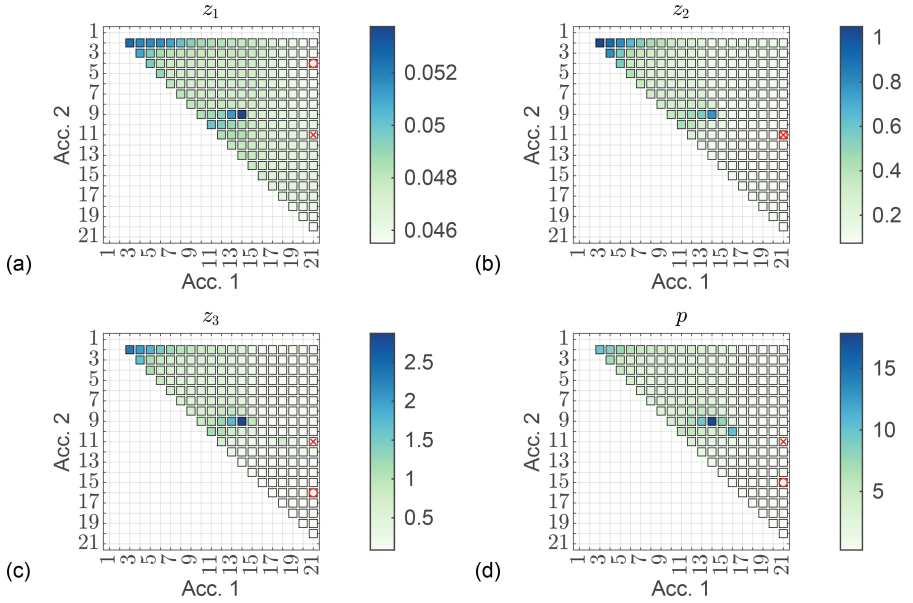

Fig. 5. Results obtained with bias-aware filtering in terms of NRMSE for the modal states (a-c) and external force (d). The red circle indicates the optimal point in each subplot, and the red cross indicates the configuration used in Sect. 3.2.

As shown in Fig. 5, many sensor configurations exist that provide good performance. Also for configurations where there is no collocated acceleration measurement, NRMSE's of below 0.5 are obtained.

While Fig. 5 testifies to the robustness of the bias-aware filter in recovering the modal states and forces, it does not give any information as to the relative improvement that can be realized with respect to a filter where modelling errors are not accounted for. To this end, Fig. 6 is presented.

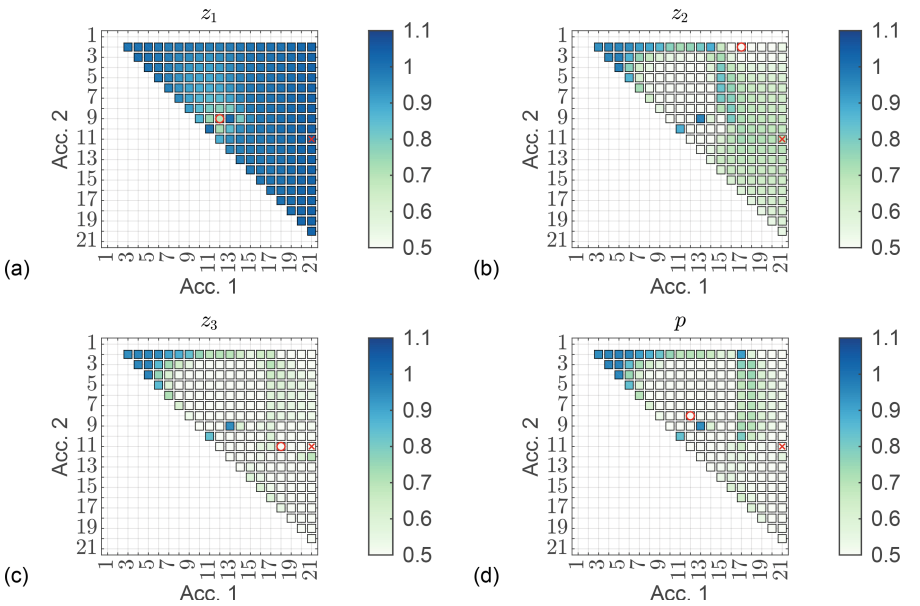

Fig. 6. Realized improvement using a bias-aware as opposed to bias-unaware filter. NRMSE for modal states (a-c) and force (d). The red circle indicates the optimal point in each subplot, and the red cross indicates the configuration used for the results in Sect. 3.2.

Figure 6 shows the NRMSE ratio between the results obtained when performing the joint input-state estimation using an erroneous model and those obtained when performing bias-aware state-input estimation. The figure illustrates the relative improvement achieved by mitigating the modelling errors. For most accelerometer locations, this ratio remains below 1, indicating a positive improvement in estimation accuracy. An exception occurs for the first modal state estimate, where the ratio is frequently close to or slightly above 1. This can most likely be attributed to the fact that the first modal state is scarcely affected by the introduced errors (cf. Figure 2a–c), making the additional bias mitigation less impactful for that mode.

4 Conclusions

A bias-aware Bayesian input-state estimator was developed, where unmodelled force residuals resulting from miscalibrated dynamic properties are estimated using a Gaussian process latent force model. Numerical examples were used to show that the developed filter is a) able to recover the underlying, true dynamics of the system, even when an unknown external force is acting on it, and b) that the identification of the external excitation greatly improves when accounting for the modelling errors using the suggested bias-aware formulation. The identification of the unknown states and input was additionally shown to be robust to changes in the sensor configuration.

References

1. Mehra RK (1970) On the identification of variance and adaptive Kalman filtering. IEEE Trans Autom Control 15(2):175–184
2. Koh CG, See LM (1994) Identification and uncertainty estimation of structural parameters. J Eng Mech 120(6):1219–1236
3. Gao Z, Gu C, Yang J, Gao S, Zhong Y (2020) Random weighting-based nonlinear Gaussian filtering. IEEE Access 8:19590–19605
4. Kim S, Deshpande VM, Bhattacharya R (2020) Robust Kalman filtering with probabilistic uncertainty in system parameters. IEEE Control Syst Lett 5(1):295–300
5. Gillijns S, De Moor B (2007) Model error estimation in ensemble data assimilation. Nonlinear Process Geophys 14(1):59–71
6. Lourens E, Fallais DJM (2019) Full-field response monitoring in structural systems driven by a set of identified equivalent forces. Mech Syst Sig Process 114:106–119
7. Yuen KV, Liang PF, Kuok SC (2013) Online estimation of noise parameters for Kalman filter. Struct Eng Mech 47(3):361–381
8. Dee DP, Da Silva AM (1998) Data assimilation in the presence of forecast bias. Q J R Meteorol Soc 124:269–295
9. Kashyap S, Rogers TJ, Nayek R (2024) A Gaussian-process assisted model-form error estimation in multiple-degrees-of-freedom systems. Mech Syst Sig Process 216:111474
10. Rogers TJ, Friis T (2022) A latent restoring force approach to nonlinear system identification. Mech Syst Sig Process 180:109426
11. Petersen ØW, Lourens E, Maes K (2024) On the impact of model errors on input and state estimation in structural dynamic systems. In: 31st International Conference on Noise and Vibration Engineering (ISMA 2024), pp 4262–4275
12. Solin A, Särkkä S (2014) Explicit link between periodic covariance functions and state space models. In: Artificial Intelligence and Statistics, pp 904–912
13. Nayek R, Chakraborty S, Narasimhan S (2019) A Gaussian process latent force model for joint input-state estimation in linear structural systems. Mech Syst Sig Process 128:479–530
14. Maes K, Smyth AW, De Roeck G, Lombaert G (2016) Joint input-state estimation in structural dynamics. Mech Syst Sig Process 70:445–466